Effect of solvent polarity on the spectroscopic properties of an alkynyl gold(I) gelator. The particular case of water.

Effect of solvent polarity on the spectroscopic properties of an alkynyl gold(I) gelator. The particular case of water

Raquel Gavara,[a,*] João Carlos Lima[b] and Laura Rodríguez[a,*]

[a] Departament de Química Inorgànica, Universitat de Barcelona, Martí i Franquès 1-11, 08028 Barcelona, Spain.

e-mail: raquel.gavara@qi.ub.es; laura.rodriguez@qi.ub.es

[b] LAQV-REQUIMTE, Departamento de Química, CQFB, Universidade Nova de Lisboa, Monte de Caparica, Portugal.

Abstract

The spectroscopic properties of aggregates obtained from the hydrogelator [Au(4-pyridylethynyl)(PTA)] were studied in solvents of different polarity. Inspection of the absorption and emission spectra of diluted solutions showed that the singlet ground state of the monomeric species is sensitive to polarity and is stabilized in more polar solvents whereas the triplet excited state is rather insensitive to changes in polarity. The study of relatively concentrated solutions revealed the presence of new emission and excitation bands at 77 K that were attributed to the presence of different kinds of aggregates. Particular interesting behaviour was observed in water where aggregation is observed to be more efficient. For this, absorption, emission quantum yields and luminescence lifetimes of water solutions at different concentrations were investigated in more detail. These data permitted to correlate the increase of non-radiative and radiative rate constants of the low lying triplet emissive state with concentration, and therefore with the low limit concentration for aggregation, due to the shortening of the Au···Au average distances in the aggregates and consequent enhancement of the spin-orbit coupling in the system.

Keywords: aggregation, gold(I), triplet states, polarity, quantum yields, lifetimes, luminescence, exciton-coupling.

1

Introduction

Luminescent materials based on transition-metal complexes receive increasing attention due to their wide application in several fields *e.g.* detection, sensing, biological labeling and displays.[1-6] In concrete, organometallic complexes represent a fascinating class of coordination compounds, which exhibit a particularly rich chemistry due to the formation of inter- and intramolecular metal–metal bonds (so-called metallophilic interactions). These interactions, together with metal-ligand coordination and additional supramolecular forces such as H-bonding, π-π interactions, and van der Waals forces among others, can originate a rich variety of metallogelators and coordination polymers.[7]

Gold(I) complexes exhibit interesting emissive properties that usually are modulated by the presence of such aurophilic (Au$\cdots$Au) interactions.[4,8-10] They are a consequence of the strong relativistic effects displayed by gold atoms and their energy can range from 20-50 kJ/mol[11,12] which is comparable to that of strong hydrogen bonds.[13] Because of its strength, aurophilicity can play a key role in molecular aggregation in both the solid state and in solution.[8,14] Although aurophilic intermolecular bonding is well documented in the solid state, the number of publications reporting on the detection of this kind of bonding in solution is still low. Due to the influence of aurophilicity in the emission properties of gold(I) complexes, luminescence become an attractive tool to study the occurrence of intermolecular aurophilic interactions in solution. Well-known is the work of Patterson and co-workers with dicyano Au(I) complex which showed a progressive red-shift[15] in the excitation band energies when increasing concentration in aqueous solutions. More recently, Li and co-workers[16] reported on a trinuclear Au(I) pyrazolate cluster exhibiting aurophilic excimeric phosphorescence as a function of concentration. In other example, Balch et al. reported on a significant variation in the emission energy of an Au(I) diaminocarbene complex in frozen solutions of several solvents which was attributed to the occurrence of aggregation.[17]

Alkynyl gold(I) complexes are an interesting family of gold(I) compounds due to their wide range of applications. The linearity imposed by the alkynyl group together with the preferential linear coordination of Au(I) and the occurrence of aurophilic contacts, make these compounds attractive building blocks for the design of emissive materials, NLO molecular materials, electronic conductors, bioimaging sensors, among others.[1,2,4,6] Moreover, they can also present interesting antiproliferative properties.[4,18] Luminescence is one of the most studied properties of these compounds and usually

2

presents a triplet state parentage, because of the heavy-atom effect of the Au(I) center that increases the possibility to observe phosphorescence at room temperature. As a consequence, the radiative and non-radiative rate constants coupling the excited triplet and singlet ground states are enhanced.[19,20] In the past, several works reported on the luminescence originated in solution by metallophilic (Au···Au, Au···Ag or Au···Cu) contacts in heterometallic-alkynyl clusters,[21-25] showing that luminescence can be a powerful tool to detect intermolecular aurophilic contacts in solution.

Recently, we reported on the auto-association properties of the alkynyl gold(I) derivative [Au(4-pyridylethynyl)(PTA)] in water.[26] This compound is able to aggregate in this solvent up to the formation of very long fibers that originate, as a last resort, a gel structure. The driving force is mainly based on the establishment of intermolecular aurophilic interactions between gold(I) atoms, as supported by relativistic density functional theory computations (Scheme 1).[27]

Related to this, it was recently found for a series of dinuclear alkynyl gold(I) derivatives ([(diphos)(AuC≡Cpy)$_2$]) (with diphosphine units containing different rigidity and chain length) a direct correlation between the Au(I)···Au(I) distance of the solids (X-ray crystal structure) and the emission quantum yields and decay times. The shortest distances gave rise to the highest radiative constants and emission quantum yields and this was attributed to the increase spin−orbit-coupling and the radiative rate constant of the lowest triplet state. Moreover, theoretical calculations predicted for these compounds a CT $\sigma^*_{Au \cdots Au}$-π^* transition which is related to the presence of aurophilic contacts.[28]

In this work, the study of the aggregation of the hydrogelator [Au(4-pyridylethynyl)(PTA)] is presented by means of the detection of the emission of potential aggregates in solvents of different polarity. Moreover, due to the particular aggregation effect observed in water, the effect of the concentration on the radiative and non-radiative deactivation channels of the excited triplet state and their connection with aggregation is also analyzed in more detail. These data will be of relevance in the analysis and understanding of other emissive supramolecular aggregates containing similar chromophoric units.
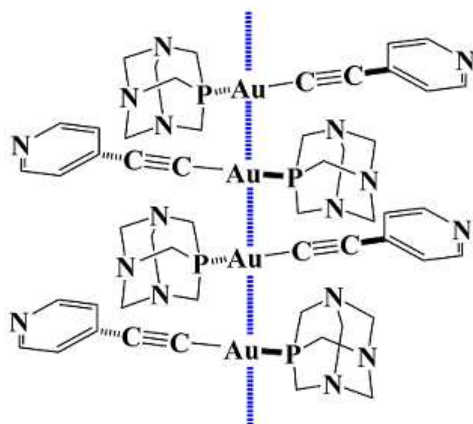
Scheme 1. Self-association of [Au(4-pyridylethynyl)(PTA)] in water.[26,27]

4

Results and Discussion

*Solvent dependence of the spectroscopic properties of compound **1**.*

The absorption spectra of 1×10^{-5} M solutions of [Au(4-pyridylethynyl)(PTA)] in several solvents of different polarity were recorded and the results are shown in Figure 1 and summarized in Table 1.
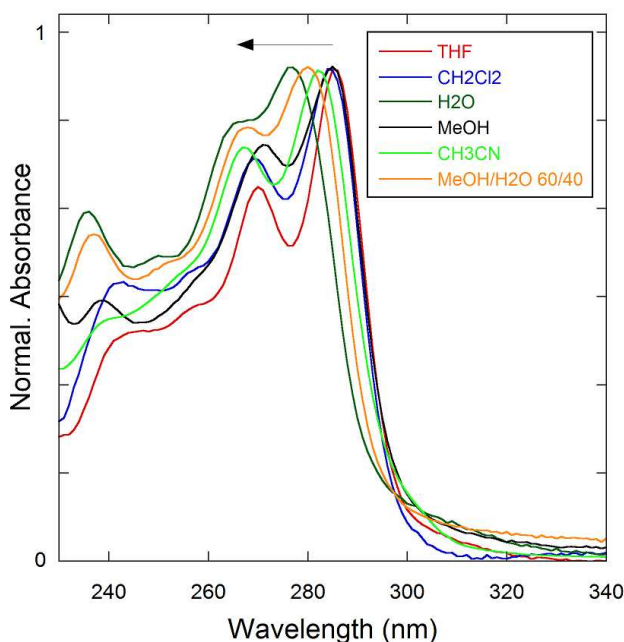

Figure 1. Normalized absorption for diluted solutions of the complex [Au(4-pyridylethynyl)(PTA)] $(1 \times 10^{-5}$ M) in several solvents at 298 K.

It can be seen that the more polar solvents induce a progressive blue shift of the absorption band. This is compatible with the existence of some charge transfer character in the intraligand $\pi\pi^*$ transition, previously assigned to the ethynylpyridine unit.[26,29] This transition shows a vibronically resolved structure with a space between maxima around 1800 cm^{-1} attributed to $\upsilon(C\equiv C)$ stretching frequencies in the excited state (Table 1).[29] In diluted solutions it is not expected significant aggregation and the recorded spectra correspond basically to the monomer. Nevertheless, it can be observed in Table 1 that the molar extinction coefficient in water is significantly lower than in the rest of solvents, which can be indicative that some aggregation already occurs in diluted solutions in this solvent. This is in agreement with the observed broadening and lower definition of the vibronic absorption band.

5

Table 1. Absorption and emission (λ_{exc} = 280 nm) data for [Au(4-pyridylethynyl)(PTA)] complex (1×10^{-5} M, 298 K) and permittivity constants (ε_r) of the solvents.

Solvent	Absorption λ_{abs} [nm] (10^{-3} ε [$M^{-1} \cdot cm^{-1}$])	Emission λ_{em} [nm]	ΔE [cm^{-1}]	ε_r
H_2O	277 (15.8), 265 (14.0)	405, 426, 438	11410	78.36
MeOH:H_2O 60:40	280 (28.6), 268 (25.3)	408, 431, 444	11204	51.67[a]
CH_3CN	282 (21.4), 267 (18.0)	408, 434, 447	10951	35.94
MeOH	285 (22.8), 271 (19.2)	411, 431, 445	10757	32.66
CH_2Cl_2	284 (20.1), 269 (16.5)	408, 429, 444	10701	8.93
THF	285 (20.6), 270 (15.7)	408, 428, 444	10578	7.58

[a] See Ref. 30.

The corresponding emissions upon excitation the samples at 280 nm display large Stokes shift (Table 1) due to a very efficient intersystem-crossing process that gives rise to the population of a less energetic triplet excited state from the more energetic singlet excited state. The emission is assigned to an intraligand $^3[\pi-\pi^*$(alkynyl)] origin (Figure 2A) and no fluorescence from the singlet excited state is observed.[26,28] The bands present a vibronic structure in all the solvents and are indicative of the ligand (C≡Cpy) orbitals participation in the emission process. In this case there is not a clear dependence of the emission maximum with the solvent nature. Interestingly, a linear dependence appears when ΔE (which is defined as the energy difference between the wavelength corresponding to the absorption maximum ($E_{\pi \to \pi^*}$) and the wavelength corresponding to the emission maximum ($E_{(\pi^*)^3 \to \pi}$)) is represented as a function of the solvent permitivity constant (Figure 2B). The data reveal the increase of ΔE with the permitivity constant, which is related to the solvent polarity. These results indicate that the triplet state is rather insensitive to the polarity of the

6

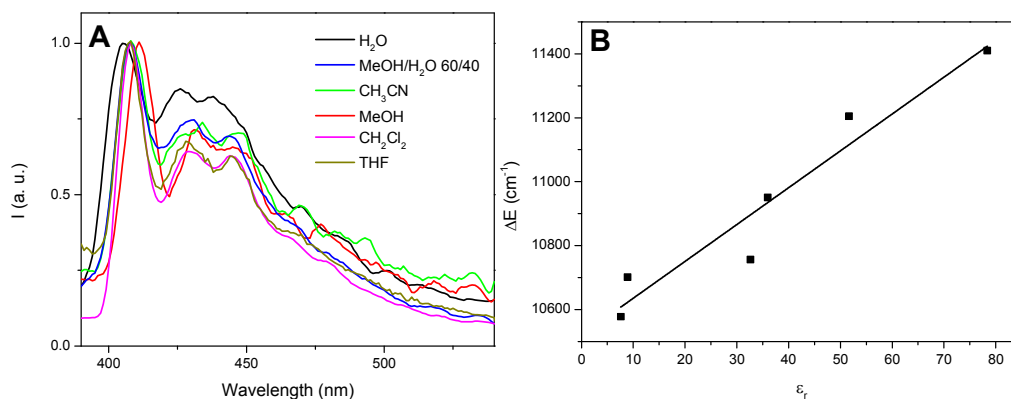solvent whereas the ground state has a polar character and is stabilized with solvent polarity.

Figure 2. (A) Normalized emission (λ_{exc} = 280 nm) for diluted solutions of [Au(4-pyridylethynyl)(PTA)] (1×10^{-5} M) in several solvents at 298 K. (B) Energy gap ΔE (defined as $E_{\pi \rightarrow \pi^*}$ - $E_{(\pi^*)^3 \rightarrow \pi}$) as a function of the solvent permitivity constant.

Relatively concentrated solutions (*ca.* 1×10^{-4} M) were also studied, in order to investigate the effect of potential intermolecular contacts in the spectroscopic properties of the compound in these solvents, due to aggregation. As a general trend, a decrease on the molar extinction coefficient at the maximum of the ethynylpyridine chromophore was observed (compare values in Table 1 and 2), and also a slight decrease in the ratio between the lowest energy and highest energy vibronic peaks (due to broadening). The most relevant cases were those concerning H_2O, MeOH/H_2O 60/40, MeOH and THF (see Figures S1 and S2 in ESI). These data are in agreement with aggregation and exciton coupling involving the ethynylpyridine chromophores, mainly, in more polar conditions.[31,32] In the particular case of THF, the different exciton splitting detected at higher concentrations seems to indicate that ethynylpyridine chromophores are interacting in the aggregates in a different way.

Table 2. Absorption data at 298 K and emission and excitation data at 77 K for aged 1×10^{-4} M solutions of [Au(4-pyridylethynyl)(PTA)] in several solvents.

Solvent	Absorption λ_{abs} [nm] (10^{-3} ε [$M^{-1} \cdot cm^{-1}$])	Emission λ_{max} (nm) (λ_{exc} = 340 nm)	Excitation λ_{max} (nm)	
H_2O	276 (10.1), 265 (10.2)	551, 476 (br), 410	λ_{em} = 570 nm	435, 380 (sh), 297
			λ_{em} = 450 nm	329, 318, 288 (sh)
			λ_{em} = 409 nm	324 (sh), 293 (sh), 276
CH_3CN	283 (21.2), 268 (18.7)	545, 477, 409	λ_{em} = 570 nm	424, 373 (sh), 311
			λ_{em} = 450 nm	336
			λ_{em} = 409 nm	320
MeOH	285 (22.5), 271 (20.6)	501, 451, 412	λ_{em} = 550 nm	411 (sh), 399
			λ_{em} = 500 nm	363, 291 (sh)
			λ_{em} = 450 nm	335, 285
			λ_{em} = 412 nm	326, 308 (sh), 285 (sh)
THF	289 (16.1), 268 (18.8)	491, 472 (sh), 411	λ_{em} = 490 nm	355, 307, 289
			λ_{em} = 409 nm	307, 289
MeOH:H_2O 60:40	280 (21.7), 268 (21.4)	479 (sh), 457, 411	λ_{em} = 510 nm	370, 294
			λ_{em} = 450 nm	333, 304 (sh), 285
			λ_{em} = 410 nm	324 (sh), 305 (sh), 288

As commented above, calculations based on similar alkynyl dinuclear gold(I) complexes predicted the existence of a charge transfer band above 300 nm assigned to a $\sigma^*_{Au\cdots Au}$-π^* transition and related to the presence of aurophilic interactions.[28] In the present case, the solutions did not present significant absorption above 300 nm in any solvent, and only presented residual emission when excited above this wavelength at room temperature. Interesting data were recorded when the samples were excited at 340 nm as frozen solutions at 77 K (Figure 3A), using front-face detection. As expected, the

non-radiative channels due to motions of the molecules or interactions solvent-solute are restricted at this temperature and the diffusion of oxygen is much slower, allowing the detection of triplet states quenched at room temperature. All the samples presented several emission bands above 400 nm: i) a higher energy and narrower band in the range 408-414 nm, comparable to that we previously assigned to an intraligand $^3[\pi–\pi^*(\text{alkynyl})]$ origin; ii) one or two broader bands at lower energies in the range 450-555 nm. The corresponding excitation spectra at 77 K show several absorption bands above 300 nm not detectable in the UV-vis absorption at room temperature (see example in Figure 3B), which are in agreement with the calculated $\sigma^*_{Au\cdots Au}$-π^* transition for analogous compounds[28] and can be associated to aggregates presenting aurophilic contacts.
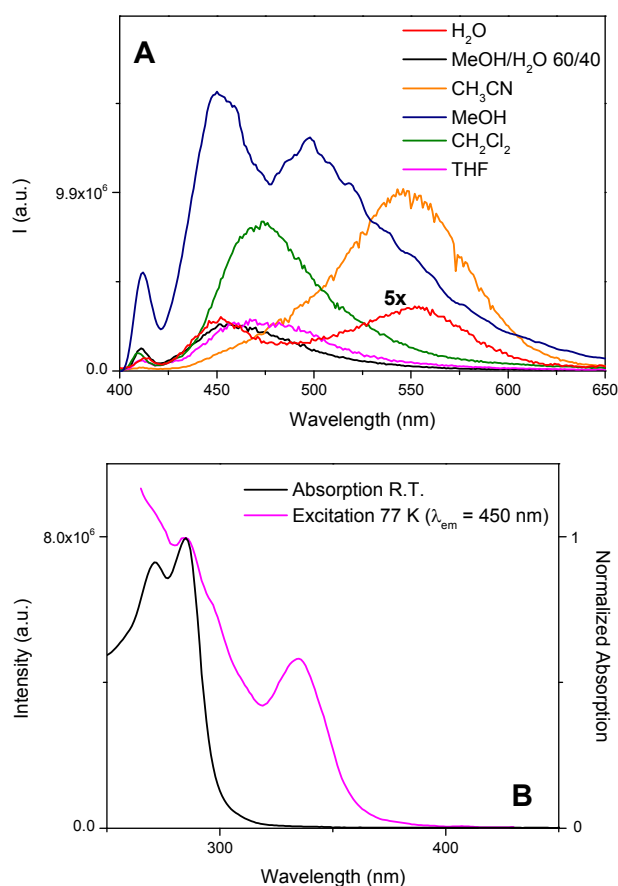

Figure 3. (A) Emission of frozen solutions of [Au(4-pyridylethynyl)(PTA)] (1×10^{-4} M, 77 K, λ_{exc} = 340 nm) in several solvents. (B) Normalized absorption at 298 K and excitation spectra at 77 K (λ_{em} = 450 nm) corresponding to the MeOH solution.

Interestingly, aging the samples for three months, leads to an increase of the emission when exciting at 340 nm (Figures S3-S6) and 77 K, in spite of the fact that not

9

significant changes are observed in the absorption spectra at room temperature.[†] Worth mentioning is the case of water where there is an increase of the emission corresponds in the case of the lowest energy emission band (λ_{max} *ca.* 550 nm), whereas there is a decrease in intensity and a red-shift of the band centered initially at 475 nm (Figure 4). The case of water is rather opposite to that observed with CH_3CN where the 475 nm band is detected only in aged samples (Figure S3). This observation seems to indicate that there is an equilibrium between species emitting at different wavelengths (different aggregates). These transitions, only observable at very low temperatures, should be originated on triplet states (see Table 2 and Figures S7-S10 for emission and excitation spectra corresponding to CH_3CN, MeOH, MeOH:H_2O 60:40 and THF).
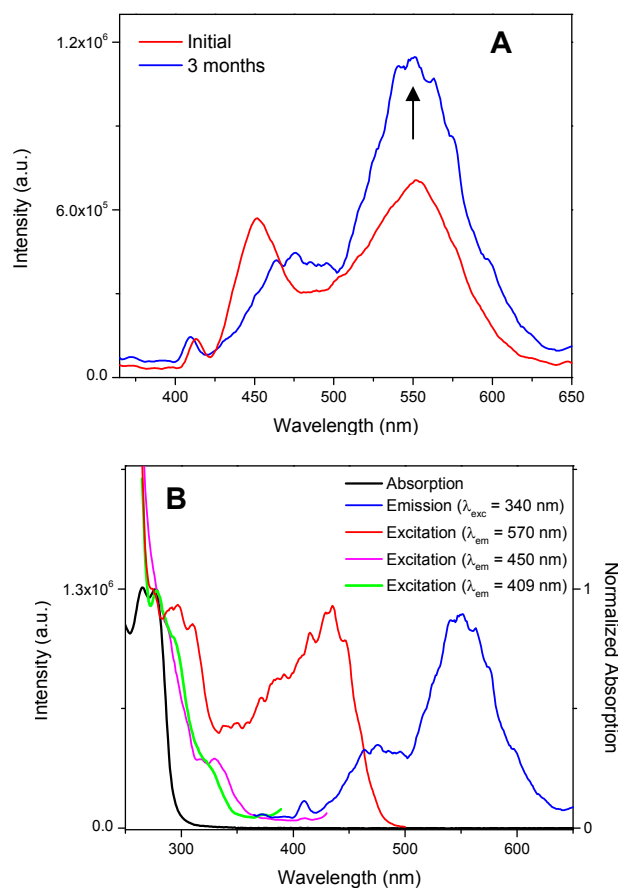

Figure 4. (A) Emission recorded at 77 K (λ_{exc} = 340 nm) for the initial and aged $1x10^{-4}$ M solution of [Au(4-pyridylethynyl)(PTA)] in water**.** (B) Normalized emission (blue,

---

[†] During this time the solutions were carefully stored, sealed and protected from light. The UV-vis absorption spectra of the samples did no change during the storage time discarding in this way decomposition of the compound. An exception was the case of CH_2Cl_2 solution, where changes in the UV-vis spectrum with a large increase in the absorption in the blue region indicated degradation of the sample, preventing the study of old solutions in this solvent.

λ_{exc} = 340 nm) and excitation spectra (red, λ_{em} = 570 nm; pink, λ_{em} = 450 nm; green, λ_{em} = 409 nm) recorded at 77 K for the aged aqueous solution of the complex. The absorption spectrum recorded at 298 K (black line) is also shown.

Omary and Elbjeirami[33] reported in 2007 on the oligomerization of an isonitrile Au(I) derivative in CH_2Cl_2 and they identified dimers and trimers in the UV-vis absorption spectra, where the absorption of the trimers was red shifted comparing with that of the dimers and the same was observed with the dimers respect to the monomers. Intuitively, we can suppose that something similar is happening in our systems and bigger aggregates containing aurophilic interactions conduct to higher red-shifts in the excitation and emission spectra. However, we cannot discard that a different packing in the aggregates (independent on the size) is responsible for the different emission and excitation bands recorded at 77 K. In fact, when we compare the emission of **1** in the solid state with the emission recorded at 77 K (Figure 5) it appears that the broad band of the solid (indicative of several environments) cover the emission recorded in the more polar solvents (water, CH_3CN and the less energetic band detected in MeOH). In the solid state it is expected to find the shortest (and strongest) Au···Au contacts which are the main driving force for the aggregation of the compound in solution.[27] By comparison, we can assume that these shorter aurophilic contacts are present in the polar solvents. Based on the charge transfer $\sigma^*_{Au\cdots Au}$-π^* transition predicted for the absorption of the aggregates and taking into account previous reports on related aggregates of platinum complexes,[3,5,34] we tentatively assigned the observed emissions to MMLCT transitions. Thus, it was reported for several platinum complexes that the stronger or more quantitative metallophillic interactions produce more pronounced red-shifted emissions from the MMLCT transitions.[35,36] Related to this, is also the work of Patterson *et al*. with dicyano Au(I) complex where higher aggregation originated lower energy transitions.[15] In our case, the most important red-shifted contribution to the emission is found in water and, for this, we assume that the occurrence of the strongest or more quantitative aurophilic interactions, and therefore the strongest aggregation, is found in water. These results are not particularly unexpected, since aurophilic contacts result from van der Waals type forces[8,11] and therefore will contribute to the hydrophobicity of the molecules in strongly polar solvents like water, leading to extensive aggregation.
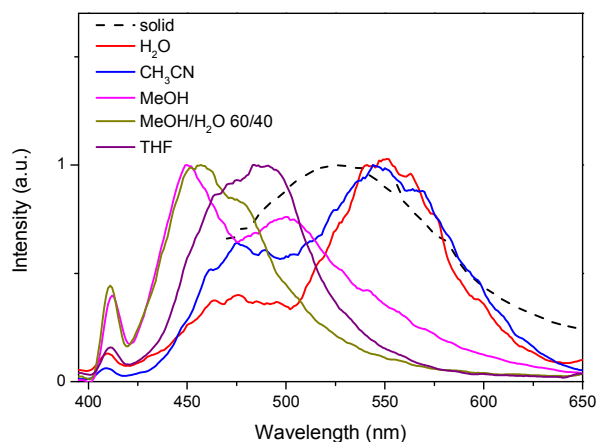
11

Figure 5. Normalized emission of [Au(4-pyridylethynyl)(PTA)] in the solid state (λ_{exc} = 410 nm, dashed line) and the aged samples of the compound at 77 K in the different solvents (λ_{exc} = 340 nm).

The impact of aggregation in the emission efficiency: the case of water.

The absorption and emission properties of a series of fresh diluted water solutions (from 2.5×10^{-6} to 3.3×10^{-5} M) of the [Au(4-pyridylethynyl)(PTA)] were measured due to the larger effect of aggregation observed in this solvent. At these conditions, it is feasible to measure the formation of aggregates in an indirect way at room temperature, because their presence will provoke a decreasing on the emission of the monomers.

The absorption spectra of the solutions are shown in Figure 6A. The broadening of the main band of the chromophore due to aggregation is clear when the ratio between the two maxima at 277 and 264 nm is plotted as a function of concentration (Figure 6B). This broadening is associated to the exciton coupling or coupling of transition moments of the ethynylpyridine chromophores when they approach to each other. The decrease in the ratio tends to stabilize for the higher concentrations and at *ca.* 3×10^{-5} M practically reaches a plateau. This means that at this concentration all the chromophores are "seeing" the same environment, *i.e.* additional aggregation is not changing the average environment detected by each chromophore.
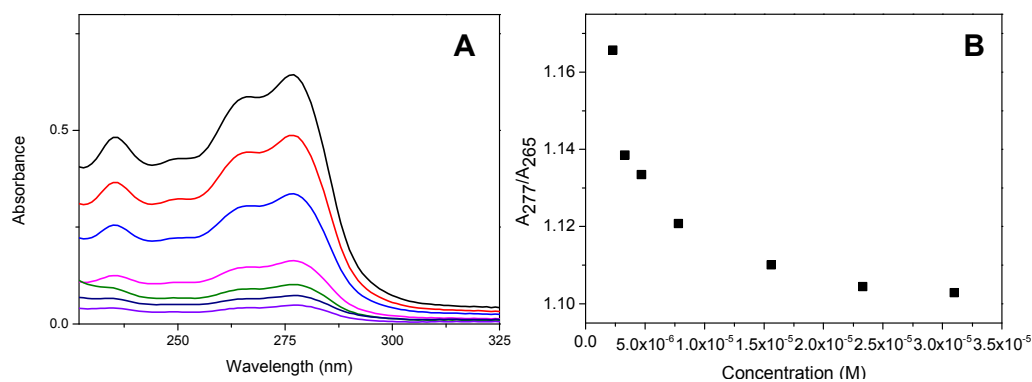
12

Figure 6. (A) Absorption spectra of [Au(4-pyridylethynyl)(PTA)] in water as a function of concentration at 298 K. (B) Ratio between the absorbances values at 277 nm *vs.* 265 nm as a function of concentration.

Emission quantum yields at room temperature were also measured for the same solutions and the results are plotted in Figure 7A and summarized in Table 3. It can be seen that in this concentration range the emission quantum yield does not change significantly with the concentration.
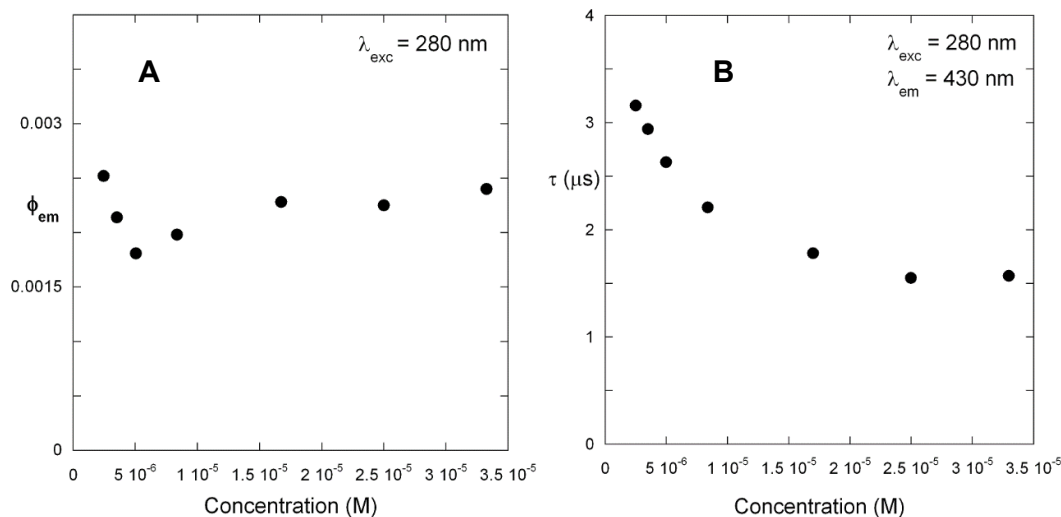

Figure 7. Emission quantum yields (A) and emission decay times (B) of [Au(4-pyridylethynyl)(PTA)] in water as a function of concentration (concentration range: 2.5×10^{-6} - 3.3×10^{-5} M, T = 298 K).

Emission decays were also collected at 430 nm upon excitation at 280 nm (Figure 8). The decays are well fitted with a scattering component and a single decay time ranging from 1.6 μs to 3.2 μs, depending on the concentration. The values of the decay times obtained for the different concentrations from the fitting of the experimental decays are plotted in Figure 7B and summarized in Table 3.

13

Table 3. Triplet emission quantum yields (λ_{exc} = 280 nm), Φ_{em}; decay times (λ_{exc} = 280 nm; λ_{em} = 430 nm), τ, radiative, k_r, and non-radiative, k_{nr}, rate constants of [Au(4-pyridylethynyl)(PTA)] complex in water at different concentrations and 298 K.

Concentration (M)	Φ_{em}	τ (μs)	k_r (μs^{-1})	k_{nr} (μs^{-1})
3.33×10^{-5}	0.0024	1.6	0.0015	0.624
2.50×10^{-5}	0.0022	1.6	0.0014	0.624
1.68×10^{-5}	0.0023	1.8	0.0013	0.554
8.38×10^{-6}	0.0012	2.2	0.0005	0.454
5.05×10^{-6}	0.0018	2.6	0.0007	0.384
3.54×10^{-6}	0.0021	2.9	0.0007	0.344
2.47×10^{-6}	0.0025	3.2	0.0008	0.312

Interestingly, while the emission quantum yield does not show any significant trend with concentration, the decay time displays a trend very similar to that found for the absorbance ratio A_{275}/A_{265} (Figure 6B) and τ becomes shorter at increasing concentrations. Thus, the decay time decreases with Au$\cdots$Au average distance (Figure 7B), as previously observed for solids where aurophilic contacts (Au$\cdots$Au distances below 3.5 Å) are present.[28]
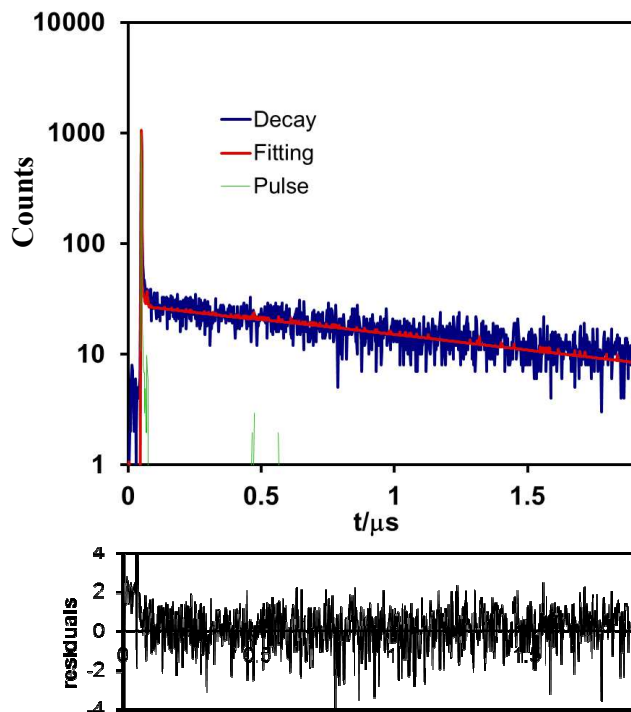
Figure 8. Emission decay (blue line) of [Au(4-pyridylethynyl)(PTA)] in water at 298 K (λ_{exc} = 280 nm; λ_{em} = 430 nm; c = 2.5x10^{-5} M). Instrument response function (blue line), fitting function (red line) and residuals are also presented.

The emission quantum yields and decay times relate to the radiative and non-radiative rate constants for the deactivation of the triplet state through Eq. (1), in which the first term of the right side is the intersystem-crossing efficiency and the second term is the triplet emission efficiency (k_r and k_{nr} stands for radiative and non-radiative rate constants of the triplet, k'_{isc} stands for inter-system crossing rate constant and k'_r and k'_{nr} stands for the singlet state deactivation constants).

$$\Phi_{em} = \frac{k'_{isc}}{k'_{isc} + k'_r + k'_{nr}} \times \frac{k_r}{k_r + k_{nr}} \tag{1}$$

As stated above, the intersystem crossing for the monomer emission at room temperature must be very efficient, since only triplet emission can be observed. As a consequence, equation 1 simplifies to the form of Eq. (2).

15

$$\Phi_{em} = \frac{k_r}{k_r + k_{nr}} \tag{2}$$

The triplet state decay times, on the other hand, are described by Eq. (3).

$$\tau = \frac{1}{k_r + k_{nr}} \tag{3}$$

From equations 2 and 3, it is straightforward to calculate both radiative and non-radiative rate constants for the triplet deactivation, and the calculated values are also summarized in Table 1 and plotted in Figure 9.
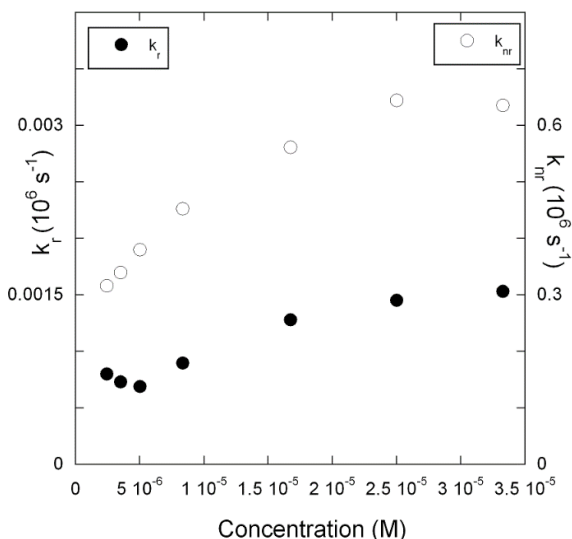

Figure 9. Concentration effect on the radiative ($\bullet$) and non-radiative ($\bigcirc$) constants from the emissive state (concentration range: 2.5×10^{-6} - 3.3×10^{-5} M) at 298 K.

Inspection of Figure 9 (and Table 3) shows that both radiative and non-radiative pathways for triplet decay increase with concentration. This trend is expected due to the decrease in the average distances between the heavy gold atoms during aggregation which will increase the intersystem crossing between the triplet excited state and the singlet ground state. As a consequence of the mixing of the gold orbitals, the $T1 \rightarrow S0$ transition becomes more allowed, as previously observed for solids where aurophilic contacts are present.[28] In this case, because of the non-radiative channel increases significantly there is no overall variation in the quantum yield.

16

Conclusions

The spectroscopic properties of the [Au(4-pyridylethynyl)(PTA)] complex are observed to be affected by solvent polarity due to different aggregation behaviour exhibited in different solvents.

In the case of the monomer, the UV-vis absorption band assigned to the ethynylpyridine chromophore presents some charge transfer character being the ground state stabilized in more polar solvents. The compound exhibits a very efficient intersystem crossing in all the solvents and the low lying excited triplet state is rather insensitive to solvent polarity.

The photophysical properties of the aggregates formed in different solvents were studied in moderately concentrated solutions (where aggregation should be more efficient). Inspection of UV-vis absorption at 298 K revealed some broadening in the band attributed to the aromatic chromophore indicating exciton coupling, which can be attributed to aggregation. Excitation spectra recorded at 77 K revealed the presence of several absorption bands above 300 nm not detectable at room temperature and tentatively assigned to triplet $\sigma^*_{Au\cdots Au}$-π^* transitions, due to the presence of several kinds of aggregates presenting aurophilic interactions. Their emission resembles that found in the compound at the solid state, especially in the case of the more polar solvents. In concrete, aged solutions in water exhibits the most red shifted emission which can be related to the presence of the strongest aurophilic contacts.

In the particular case of water, aggregation produces a noticeable increase in the intersystem-crossing to the singlet ground state and increases both radiative and non-radiative rate constants. This is directly related to the approaching of gold atoms and establishment of aurophilic interactions. These interactions seem to be already established at 3×10^{-5} M where the increase in the radiative and non-radiative constants reaches a plateau.

17

Experimental

General Procedures. Synthesis of [Au(4-pyridylethynyl)(PTA)] complex was reported elsewhere.[26]

Physical Measurements.

Solutions were prepared with Millipore water and spectroscopic grade solvents. Absorption spectra were acquired on a Varian Cary 100 Bio spectrophotometer. Emission and excitation spectra were recorded on a Horiba−Jobin−Yvon SPEX Fluorolog 3.22 and Nanolog spectrofluorimeters. Measurements of the frozen solutions at 77 K were carried out with the samples contained in a quartz tube inside a quartz-walled Dewar filled with liquid nitrogen, using front-face detection. Emission quantum yields at 298 K were measured by employing tryptophan as reference (ϕ_F = 0.14, pH 7.2)[37] for the excitation of the samples at 280 nm.

Emission decays were measured via the Time Correlated Single Photon Counting technique (TCSPC) using a home-built equipment. The samples were excited at 280 nm using a nanoled (IBH).The electronic start pulses were shaped in a constant fraction discriminator (Canberra 2126) and directed to a time to amplitude converter (TAC, Canberra 2145). Emission wavelength (430 nm) was selected by a monochromator (Oriel 77250) imaged in a fast photomultiplier (9814B Electron Tubes Inc.), the PM signal was shaped as before and delayed before entering the TAC as stop pulses. The analogue TAC signals were digitized (ADC, ND582) and stored in multichannel analizer installed in a PC (1024 channels, 1.95 ns/ch).

Acknowledgements

References

[1] V. W.-W. Yam and E. C.-C. Cheng, Highlights on the recent advances in gold chemistry-a photophysical perspective, *Chem. Soc. Rev.*, 2008, **37**, 1806-1813.

[2] G.-J. Zhou and W.-Y. Wong, Organometallic acetylides of Pt^{II}, Au^{I} and Hg^{II} as new generation optical power limiting materials, *Chem. Soc. Rev.*, 2011, **40**, 2541-2566.

[3] M. Mauro, A. Aliprandi, D. Septiadi, N.S. Kehra and L. De Cola, When self-assembly meets biology: luminescent platinum complexes for imaging applications, *Chem. Soc. Rev.*, 2014, **43**, 4144-4166.

[4] J. C. Lima and L. Rodríguez, Applications of gold(I) alkynyl systems: a growing field to explore, *Chem. Soc. Rev.*, 2011, **40**, 5442-5456.

[5] A. Aliprandi, D. Genovese, M. Mauro and L. De Cola, Recent Advances in Phosphorescent Pt(II) Complexes Featuring Metallophilic Interactions: Properties and Applications, *Chem. Lett.*, 2015, **44**, 1152–1169.

[6] E. E. Langdon-Jones and S. J. A. Pope, Recent developments in gold(I) coordination chemistry: luminescence properties and bioimaging opportunities, *Chem. Commun.*, 2014, **50**, 10343-10354.

[7] J. Zhang, C.-Y. Su, Metal-organic gels: From discrete metallogelators to coordination polymers, *Coord. Chem. Rev.*, 2013, **257**, 1373-1408.

[8] H. Schmidbaur, A. Schier, Aurophilic interactions as a subject of current research: an up-date, *Chem. Soc. Rev.*, 2012, **41**, 370-412.

[9] X. M. He and V. W.-W. Yam, Luminescent Gold(I) Complexes for Chemosensing, *Coord. Chem. Rev.*, 2011, **255**, 2111-2123.

[10] V. W. W. Yam and K. M. C. Wong, Luminescent metal complexes of d^6, d^8 and d^{10} transition metal centres, *Chem. Commun.*, 2011, **47**, 11579-11592.

[11] P. Pyykkö, Strong Closed-Shell Interactions in Inorganic Chemistry, *Chem. Rev.*, 1997, **97**, 597-636.

[12] H. Schmidbaur, W. Graf and G. Müller, Weak Intramolecular Bonding Relationships: The Conformation-Determining Attractive Interaction between Gold(I) Centers, *Angew. Chem. Int. Ed. Engl.*, 1988, **27**, 417-419.

[13] T. Steiner, The hydrogen bond in the solid state, *Angew. Chem. Int. Ed.*, 2002, **41**, 49-76.

[14] J. C. Lima and L. Rodríguez, Supramolecular Gold Metallogelators: The Key Role of Metallophilic Interactions, *Inorganics*, 2015, **3**, 1-18.

[15] M. A. Rawashdeh-Omary, M. A. Omary and H. H. Patterson, Oligomerization of $Au(CN)_2^-$ and $Ag(CN)_2^-$ Ions in Solution via Ground-State Aurophilic and Argentophilic Bonding, *J. Am. Chem. Soc.*, 2000, **122**, 10371-10380.

[16] W.-X. Ni, M. Li, J. Zheng, S. Z. Zhan, Y.-M. Qiu, S. W. Ng and D. Li, Approaching White-Light Emission from a Phosphorescent Trinuclear Gold(I) Cluster by Modulating Its Aggregation Behavior, *Angew. Chem. Int. Ed.*, 2013, **52**, 13472 –13476.

[17] R. L. White-Morris, M. M. Olmstead, F. Jiang, D. S. Tinti and A. L. Balch, Remarkable Variations in the Luminescence of Frozen Solutions of [Au{C(NHMe)2}2](PF6)·0.5(Acetone). Structural and Spectroscopic Studies of the Effects of Anions and Solvents on Gold(I) Carbene Complexes, *J. Am. Chem. Soc.*, 2002, **124**, 2327-2336.

[18] E. Vergara, E. Cerrada, A. Casini, O. Zava, M. Laguna and P. J. Dyson, Antiproliferative Activity of Gold(I) Alkyne Complexes Containing Water-Soluble Phosphane Ligands, *Organometallics*, 2010, **29**, 2596-2603.

[19] I. O. Koshevoy, Y.-C. Chang, A. J. Karttunen, M. Haukka, T. Pakkanen and P.-T. Chou, Modulation of Metallophilic Bonds: Solvent-Induced Isomerization and Luminescence Vapochromism of a Polymorphic Au−Cu Cluster, *J. Am. Chem. Soc.*, 2012, **134**, 6564−6567.

[20] I. O. Koshevoy, Y.-C. Chang, A. J. Karttunen, J. R. Shakirova, J. Jänis, M. Haukka, T. Pakkanen and P.-T. Chou, Solid-State Luminescence of Au-Cu-Alkynyl Complexes Induced by Metallophilicity-Driven Aggregation, *Chem. Eur. J.*, 2013, **19**, 5104 – 5112.

[21] G. F. Manbeck, W. W. Brennessel, R. A. Stockland Jr. and R. Eisenberg, Luminescent Au(I)/Cu(I) Alkynyl Clusters with an Ethynyl Steroid and Related Aliphatic Ligands: An Octanuclear Au_4Cu_4 Cluster and Luminescence Polymorphism in Au_3Cu_2 Clusters, *J. Am. Chem. Soc.*, 2010, **132**, 12307–12318.

[22] I. O. Koshevoy, Y.-C. Lin, A. J. Karttunen, M. Haukka, P.-T. Chou, S. P. Tunik and T. A. Pakkanen, An intensely and oxygen independent phosphorescent gold(I)–silver(I) complex: ''trapping'' an Au_8Ag_{10} oligomer by two gold-alkynyl-diphosphine molecules, *Chem. Commun.*, 2009, **45**, 2860–2862.

[23] I. O. Koshevoy, Y.-C. Lin, Y.-C. Chen, A. J. Karttunen, M. Haukka, P.-T. Chou, S. P. Tunik and T. A. Pakkanen, Rational reductive fusion of two heterometallic clusters: formation of a highly stable, intensely phosphorescent Au–Ag aggregate and application in two-photon imaging in human mesenchymal stem cells, *Chem. Commun.*, 2010, **46**, 1440–1442.

[24] X. He, N. Zhu and V. W.-W. Yam, Design and synthesis of luminescence chemosensors based on alkynyl phosphine gold(I)–copper(I) aggregates, *Dalton Trans.*, 2011, **40**, 9703-9710.

[25] I. O. Koshevoy, P. V. Ostrova, A. J. Karttunen, A. S. Melnikov and M. A. Khodorkovskiy, Assembly of the heterometallic Au(I)–M(I) (M= Cu, Ag) clusters containing the dialkyne-derived diphosphines: synthesis, luminescence and theoretical studies, *Dalton Trans.*, 2010, **39**, 9022–9031.

[26] R. Gavara, J. Llorca, J. C. Lima and L. Rodríguez, A luminescent hydrogel based on a new Au(I) complex, *Chem. Commun.*, 2013, **49**, 72-74

[27] R. Gavara, E. Aguiló, C. Fonseca Guerra, L. Rodríguez and J. C. Lima, Thermodynamic Aspects of Aurophilic Hydrogelators, *Inorg. Chem.*, 2015, **54**, 5195-5203.

[28] L. Rodríguez, M. Ferrer, R. Crehuet, J. Anglada and J. C. Lima, Correlation between Photophysical Parameters and Gold−Gold Distances in Gold(I) (4-Pyridyl)ethynyl Complexes, *Inorg. Chem.*, 2012, **51**, 7636-7641.

[29] M. Ferrer, A. Gutiérrez, L. Rodríguez, O. Rossell, J. C. Lima, M. Font-Bardía and X. Solans, Study of the Effect of the Phosphane Bridging Chain Nature on the Structural and Photophysical Properties of a Series of Gold(I) Ethynylpyridine Complexes, *Eur. J. Inorg. Chem.*, 2008, 2899-2909.

[30] P. S. Albright and L. J. Gosting, Dielectric Constants of the Methanol-Water System from 5 to 55°, *J. Am. Chem. Soc.*, 1946, **68**, 1061-1063.

[31] E. G. McRae and M. Kasha, Enhancement of Phosphorescence Ability upon Aggregation of Dye Molecules, *J. Chem. Phys.*, 1958, **28**, 721-722.

[32] M. Kasha, H. R. Rawls and M. A. El-Bayoumi, The exciton model in molecular spectroscopy, *Pure Appl. Chem.*, 1965, **11**, 371-392.

[33] O. Elbjeirami and M. A. Omary, Photochemistry of Neutral Isonitrile Gold(I) Complexes: Modulation of Photoreactivity by Aurophilicity and π-Acceptance Ability, *J. Am. Chem. Soc.*, 2007, **129**, 11384-11393.

[34] K.M.-C. Wong and V.W.-W. Yam, Self-Assembly of Luminescent Alkynylplatinum(II) Terpyridyl Complexes: Modulation of Photophysical Properties through Aggregation Behavior, *Accounts Chem. Res.*, 2011, **44**, 424-434.

[35] V.W.-W. Yam, K.H.-Y. Chan, K.M.-C. Wong and N. Zhu, Luminescent Platinum(II) Terpyridyl Complexes: Effect of Counter Ions on Solvent-Induced Aggregation and Color Changes, *Chem. Eur. J.*, 2005, **11**, 4535 – 4543.

[36] C. Yu, K. H.-Y. Chan, K. M.-C. Wong and V. W.-W. Yam, Polyelectrolyte-Induced Self-Assembly of Positively Charged Alkynylplatinum(II)–Terpyridyl Complexes in Aqueous Media, *Chem. Eur. J.*, 2008, **14**, 4577-4584.

[37] E. P. Kirby and R. F. Steiner, Influence of solvent and temperature upon the fluorescence of indole derivatives, *J. Phys. Chem.*, 1970, **74**, 4480-4490.

GRAPHICAL ABSTRACT

The spectroscopic properties of an aurophilic hydrogelator depend on solvent polarity and concentration.
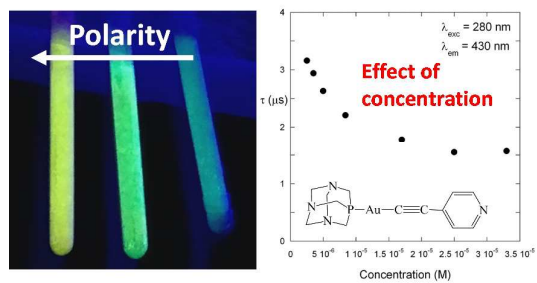
Effect of solvent polarity on the spectroscopic properties of an alkynyl gold(I) gelator. The particular case of water

Raquel Gavara,[a,*] João Carlos Lima[b] and Laura Rodríguez[a,*]

[a] Departament de Química Inorgànica, Universitat de Barcelona, Martí i Franquès 1-11, 08028 Barcelona, Spain.

e-mail: raquel.gavara@qi.ub.es; laura.rodriguez@qi.ub.es

[b] LAQV-REQUIMTE, Departamento de Química, CQFB, Universidade Nova de Lisboa, Monte de Caparica, Portugal.

Supplementary Information
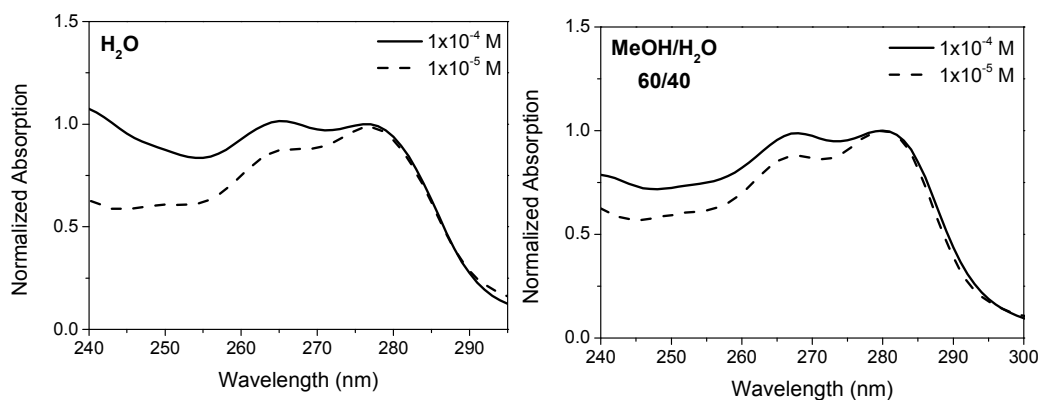
Figure S1. Normalized UV-vis absorption spectra at 298 K corresponding to 1×10^{-4} M (solid line) and 1×10^{-4} M (dashed line) solutions of [Au(4-pyridylethynyl)(PTA)] in H$_2$O (left) and MeOH/ H$_2$O 60/40 (right).
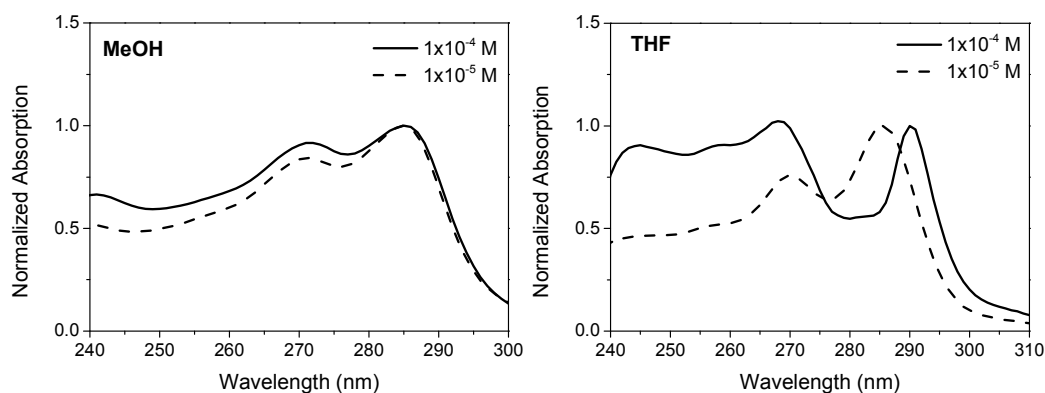
Figure S2. Normalized UV-vis absorption spectra at 298 K corresponding to 1×10^{-4} M (solid line) and 1×10^{-4} M (dashed line) solutions of [Au(4-pyridylethynyl)(PTA)] in MeOH (left) and THF (right).
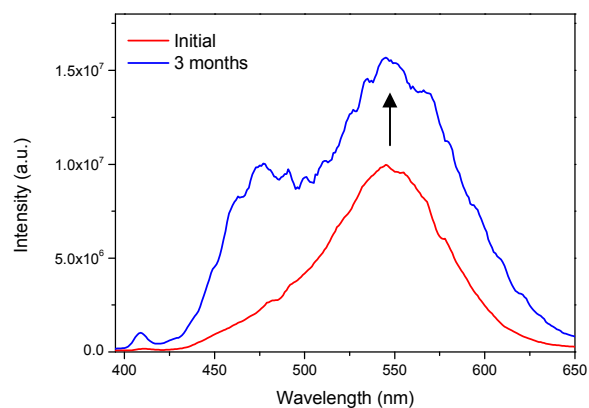
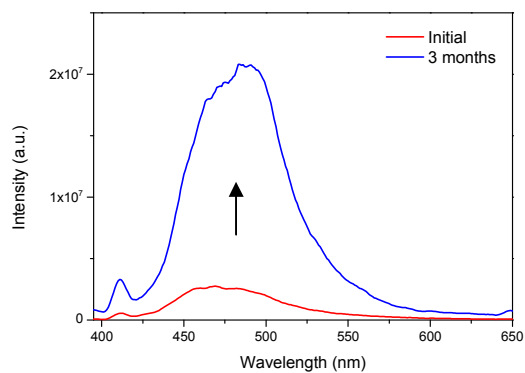**Figure S3.** Emission recorded at 77 K (λ_{exc} = 340 nm) for the initial and aged $1x10^{-4}$ M solution of [Au(4-pyridylethynyl)(PTA)] in CH_3CN.
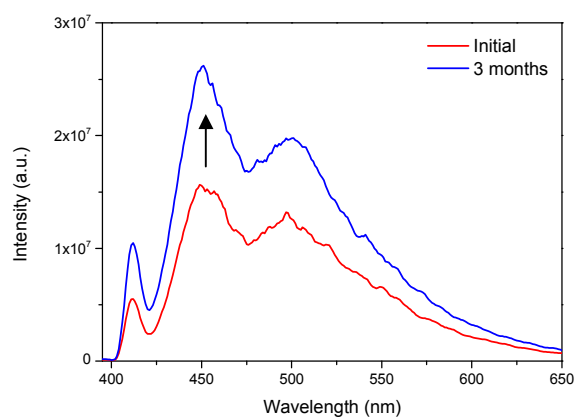
Figure S4. Emission recorded at 77 K (λ_{exc} = 340 nm) for the initial and aged $1x10^{-4}$ M solution of [Au(4-pyridylethynyl)(PTA)] in MeOH.
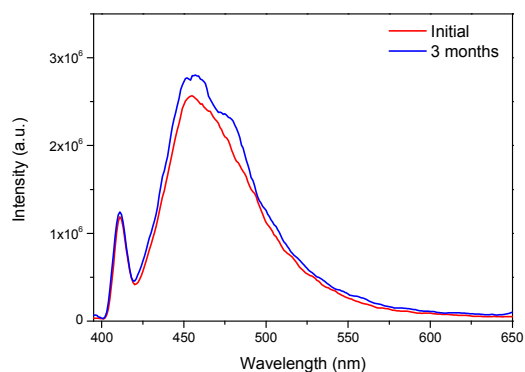
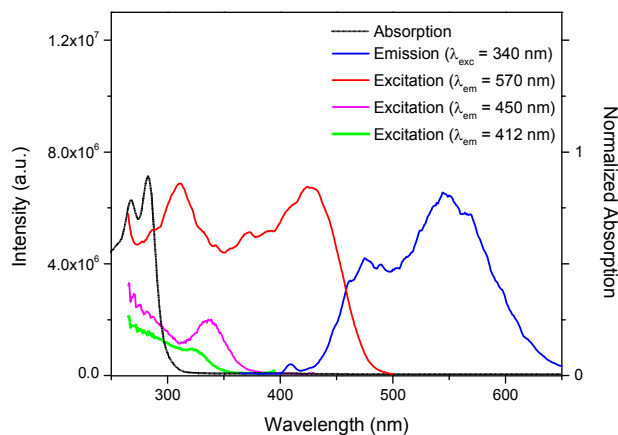**Figure S5.** Emission recorded at 77 K (λ_{exc} = 340 nm) for the initial and aged 1×10^{-4} M solution of [Au(4-pyridylethynyl)(PTA)] in MeOH/H$_2$O 60/40**.**

Figure S6. Emission recorded at 77 K (λ_{exc} = 340 nm) for the initial and aged 1×10^{-4} M solution of [Au(4-pyridylethynyl)(PTA)] in THF.

Figure S7. Normalized emission (blue, λ_{exc} = 340 nm) and excitation spectra (red, λ_{em} = 570 nm; pink, λ_{em} = 450 nm; green, λ_{em} = 412 nm) recorded at 77 K for the aged CH_3CN solution of [Au(4-pyridylethynyl)(PTA)]. The absorption spectrum recorded at 298 K (black line) is also shown.
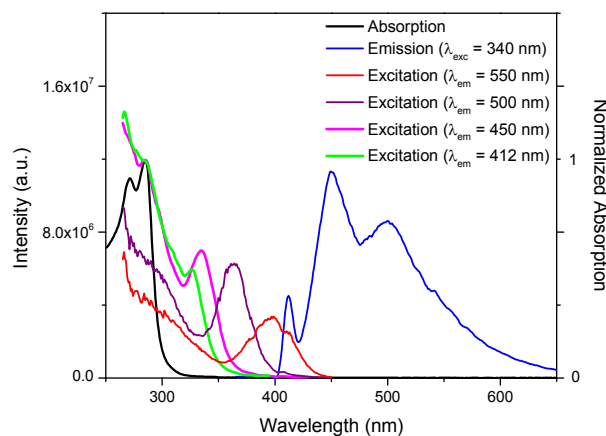

Figure S8. Normalized emission (blue, λ_{exc} = 340 nm) and excitation spectra (red, λ_{em} = 550 nm; purple, λ_{em} = 500 nm; pink, λ_{em} = 450 nm; green, λ_{em} = 412 nm) recorded at 77 K for the aged MeOH solution of [Au(4-pyridylethynyl)(PTA)]. The absorption spectrum recorded at 298 K (black line) is also shown.

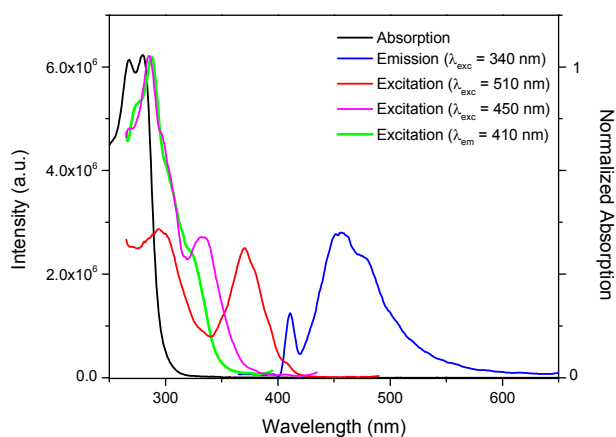**Figure S9.** Normalized emission (blue, λ_{exc} = 340 nm) and excitation spectra (red, λ_{em} = 510 nm; pink, λ_{em} = 450 nm; green, λ_{em} = 410 nm) recorded at 77 K for the aged MeOH/H$_2$O 60/40 solution of [Au(4-pyridylethynyl)(PTA)]**.** The absorption spectrum recorded at 298 K (black line) is also shown.
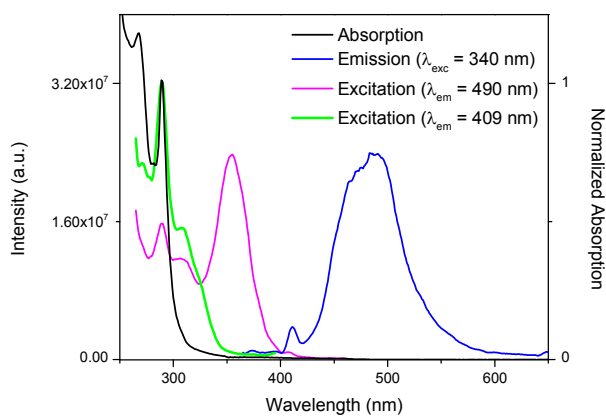

Figure S10. Normalized emission (blue, λ_{exc} = 340 nm) and excitation spectra (pink, λ_{em} = 490 nm; green, λ_{em} = 409 nm) recorded at 77 K for the aged THF solution of [Au(4-pyridylethynyl)(PTA)]. The absorption spectrum recorded at 298 K (black line) is also shown.